Stability and phonons of $KTaO_3$

David J. Singh
Complex Systems Theory Branch, Naval Research Laboratory, Washington, DC 20375
(Received 16 June 1995)

$KTaO_3$ was investigated using density functional methods. These local-density approximation calculations correctly show the absence of a ferroelectric instability in this compound. Phonon frequencies and bulk properties in good agreement with existing measurements are obtained. A highly anharmonic low-frequency mode corresponding to the observed incipient ferroelectric behavior is identified. The electronic structure shows strong transition metal oxygen covalency as in known ferroelectric perovskites. As expected properties show a strong similarity with $KNbO_3$. The absence of ferroelectricity in $KTaO_3$ is due to the extreme sensitivity of the soft mode to the covalency and the slight chemical differences of Nb and Ta, particularly the higher *d* binding energy in Nb.

INTRODUCTION

Ferroelectric and related perovskites have been the subject of extensive investigation, both because of their technical importance and because of fundamental interest in the physics of their phase transitions.[1] These materials have chemical formulas ABO_3. The ideal structure is cubic perovskite, where the A and B cations are arranged on a simple cubic lattice (as in CsCl structure), and the O ions lie on the face centers nearest the (typically transition metal) B cations. Thus the B cations are at the center of O octahedra, while the A cations lie in a larger 12-fold coordinated site. This ideal structure displays a wide variety of structural instabilities in the various materials. These may involve rotations and distortions of the O octahedra as well as displacements of the cations from their ideal sites. The interplay of these instabilities accounts for the rich variety of ferroelectric and antiferroelectric behaviors.

The $K(Nb_{1-x}Ta_x)O_3$ pseudobinary alloy (KTN) is among the most extensively studied systems in this class. Despite the very similar chemistry of Nb and Ta, the two end points display quite different behavior. Conversely, the origin of the ferroelectricity in KTN must be extremely sensitive to the properties of the B site cation.

$KNbO_3$ has a series of ferroelectric phase transitions, starting with the cubic to tetragonal transition at 710 K, followed by a tetragonal to orthorhombic transition and finally settling into a rhombohedral ferroelectric ground state. The ground state structure[2] is derived from the cubic perovskite structure by opposing shifts of the Nb and O atoms, the Nb atoms along a cube axis and the larger O shifts roughly along the same axis.

In contrast, $KTaO_3$ is described as an incipient ferroelectric; its structure remains cubic perovskite down to low temperature.[3] There is a softening transverse optic (TO) phonon corresponding to the ferroelectric mode in $KNbO_3$, but its frequency remains finite at all temperatures.[4–6] Ferroelectricity can be induced by uniaxial stress or very low level doping on either the K or Ta sites. Nb impurities, even at extremely low concentrations, result in local dipoles, which could be regarded as locally ferroelectric regions. These couple yielding ferroelectric-like behavior for Nb concentrations above 1% (the precise nature for low concentrations is somewhat controversial).[7–9]

There have been several first principles studies of the structure and phonons of the KTN system, primarily for the $KNbO_3$ end point.[10–17] As emphasized by Cohen and Krakauer,[18,19] the bonding of these materials is strongly affected by transition metal-oxygen hybridization, so that description of the ferroelectric modes involves a very delicate balance between covalent, Coulomb, and repulsive ionic interactions.

Singh and Boyer[10] performed local-density approximation (LDA) calculations using the linearized augmented plane-wave (LAPW) method for $KNbO_3$. As is typical in LDA calculations, they obtained a lattice parameter slightly smaller than the experimental value, in this case by 1.3%. Very good agreement with experimental data was obtained for the stable phonon frequencies at Γ. Moreover, a zone center (Γ) TO ferroelectric mode was identified. This mode showed a strong volume dependence, being essentially stable at the LDA lattice parameter, but unstable at the larger experimental volume. No unstable modes were found at the *R* point. This shows that the ferroelectric mode requires a correlated motion of the atoms, and that there is no instability against arbitrary patterns of Nb displacements.

The magnitude of the ferroelectric displacement, as calculated by minimizing the total energies, was within 20% of the experimental value, and the calculated eigenvector was in close agreement with the experimental rhombohedral structure. The energetics of the ferroelectric instability are sensitive to the Brillouin zone sampling,[20,11] reflecting the importance of covalency. Converged calculations[11] yield an instability energy of 2.3 mRy/cell at the experimental volume. The finding of a ferroelectric instability in good agreement with experiment is gratifying since LDA calculations generally agree best with experiment when performed at the experimental lattice parameter. However, the high sensitivity to the volume does pose problems for the use of the LDA as a predictive tool in this system, since the ferroelectric instability is suppressed at the calculated volume. Generalized gradient approximation (GGA) calculations[11] yield very similar results for the ferroelectric mode and its volume dependence, but the equilibrium lattice parameter is increased

to a value slightly larger than experiment.

Yu and co-workers[14] have used linear response calculations to perform considerably more extensive studies of the phonons in $KNbO_3$. The results at the Γ and R points are in general agreement with those of Singh and Boyer, both regarding the frequencies and eigenvectors. These seminal calculations additionally showed the presence of slabs of unstable phonons in reciprocal space, and thereby provided understanding of the phase transitions and a physical basis for the eight-sites picture of Comes, Lambert, and Guinier.[21]

Postnikov and co-workers (P) (Refs. 12,13) performed a series of LDA calculations using the linearized muffin tin orbital method (LMTO) for both $KNbO_3$ and $KTaO_3$. For $KNbO_3$ in the cubic perovskite structure they obtain a lattice parameter 1.7% smaller than experiment, and phonon frequencies at the experimental volume in reasonable agreement with those of Refs. 9 and 13. Significant differences are that in their calculations $KNbO_3$ is unstable both at the LDA volume and the larger experimental volume, $KNbO_3$ is unstable against displacement of a single Nb atom and the calculated displacement pattern differs both from previous calculations and experiment. The instability against motion of single Nb atoms, which they found in supercell calculations, implies unstable phonons throughout the Brillouin zone, in contradiction particularly with the results of Yu and coworkers and the resulting elegant explanation of the diffraction experiments of Comes *et al.* and the phase transitions.

As mentioned, P have also reported LDA calculations for $KTaO_3$. In this case, they obtain a lattice parameter 1.4% smaller than experiment. At the experimental lattice parameter, they find a ferroelectric instability as well as an instability against displacement of the Ta atoms alone, while at the smaller LDA lattice parameter all zone center phonons are stable. As in $KNbO_3$, the eigenvectors differ significantly from experiment.[6] It seems that additional LDA calculations of the phonons and the degree of stability against ferroelectricity for $KTaO_3$ are needed.

Here I present the results of a series of well converged LDA calculations for $KTaO_3$. The results are similar to those of P in most regards, but differ significantly for the ''ferroelectric'' mode. This reflects the delicate balance of various contributions and the resulting high sensitivity of the ferroelectric mode to its treatment in calculations as well as to physical and chemical modifications. The present results are, however, in general accord with expectations based on prior calculations for $KNbO_3$. In particular, calculated phonon frequencies and eigenvectors are in good accord with experiment, which bodes well for the use of LDA calculations to analyze the technologically important KTN alloy system.

APPROACH

The present calculations were performed within the LDA using a local orbital extension[22] of the general potential LAPW method.[23,24] This method has a flexible basis in all regions of space and makes no shape approximations to either the density or potential. As such it is well suited to open, low symmetry crystal structures such as the distorted perovskites considered here. Further, with the local orbital extension, high lying core states and valence states may both be treated in a single energy window, without compromising the accuracy. This and the more flexible basis in the interstitial region are significant differences from the full-potential linearized muffin tin orbital method used in Refs. 12 and 13. The present calculations were performed using the Hedin-Lundqvist parametrization of the LDA.[25]

Brillouin zone samplings were performed using the special points method. $6\times6\times6$ meshes were used for the cubic perovskite structure and the Γ_{25} (see below) phonon mode. More dense $8\times8\times8$ meshes were used for the three Γ_{15} modes including the ''ferroelectric'' mode. Well converged basis sets, consisting of approximately 825 LAPW functions plus local orbitals were employed. The local orbitals were used to include the upper extended core states (Ta $5s$, $5p$, and $4f$, O $2s$, and K $3s$, and $3p$) as well as to relax the linearization of the Ta $5d$ state. Both the valence and core states were treated self-consistently, the core states relativistically and the valence states in a scalar relativistic approximation. Forces were calculated using the method of Yu, Singh, and Krakauer.[26] These were used to determine the phonon frequencies and eigenvectors for the three Γ_{15} modes.

CUBIC PEROVSKITE STRUCTURE

The LDA lattice parameter and bulk modulus were determined by the standard approach of calculating the total energy as a function of lattice parameter and fitting the results with the Birch equation of state. In this way a lattice parameter of 3.96 Å or 0.6% smaller than experiment is obtained, with a bulk modulus of 211 GPa at the LDA lattice parameter. Adjusted to the experimental lattice parameter, as should be done to obtain reliable elastic properties from LDA calculations, the calculated bulk modulus is 196 GPa, which is 10% below the experimental value of 218 GPa as determined from elastic constants.[27,28] The differences from the work of P are also quite small. They obtained a lattice parameter of 3.93 Å (1.3% below experiment) and a bulk modulus of 225 GPa.

The electronic structure of $KTaO_3$ is very similar to that of $KNbO_3$, as may be expected. This is illustrated by comparison of the band structure with that obtained by parallel calculations for $KNbO_3$ (Fig. 1). These band structures are qualitatively like those of a previous study[29] that employed the LMTO method within the atomic sphere approximation (ASA). However, the details of the dispersion differ by about 1 eV in places. This is to be expected since the ASA is not reliable for materials with open structures and low site symmetries, such as perovskites. Roughly speaking, the nine valence bands are derived from the O $2p$ orbitals. These are separated by an indirect (R-Γ) gap from the transition metal d derived conduction bands. However, there is quite strong p-d hybridization, as is evident from the sphere projected density of states (DOS). This is shown for $KTaO_3$ in Fig. 2 (the $KNbO_3$ DOS is almost identical and is not reproduced). The Ta $5d$ contribution is zero at the valence band maximum, but rises strongly with increasing binding energy. Conversely, the O $2p$ contribution rises from zero at the conduction band minimum with increasing energy. This reflects the Ta $5d-$O $2p$ covalency.

The significant differences between the calculated band structures of $KNbO_3$ and $KTaO_3$ are a 0.6 eV larger band gap

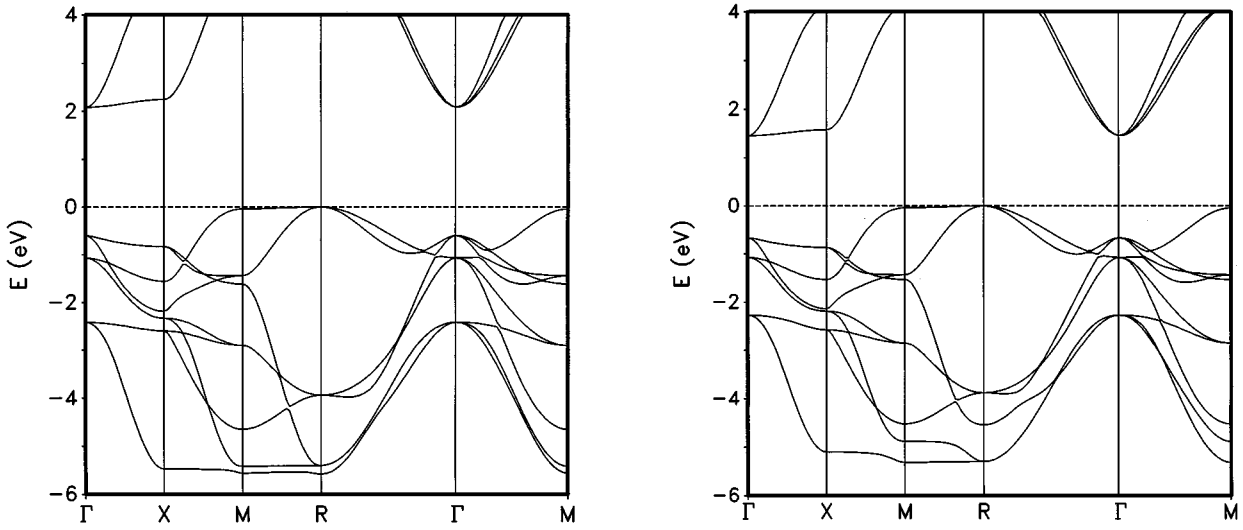

FIG. 1. Calculated electronic band structures of $KTaO_3$ (left) and $KNbO_3$ (right) in the cubic perovskite structure.

in the tantalate, and a considerably stronger dispersion of one of the bands between M and R. This singly degenerate band is the lowest band at R in $KTaO_3$, but is 1 eV higher in $KNbO_3$. The dispersion of this O $2p$ derived band (unlike the other bands in this energy region its symmetry does not admit any Ta $5d$ character), reflects O-O interactions, which are evidently larger in $KTaO_3$. These may arise either directly, or indirectly through the Ta $6s$ orbital. The transition metal d O p interactions, which are reflected in the nearly identical conduction band dispersions and the dispersions of the d-p hybridized valence bands are practically identical in $KNbO_3$ and $KTaO_3$. As is typical in LDA calculations for oxides, the band gaps are underestimated. The experimental gaps are 3.3 eV for $KNbO_3$ and 3.8 eV for $KTaO_3$.

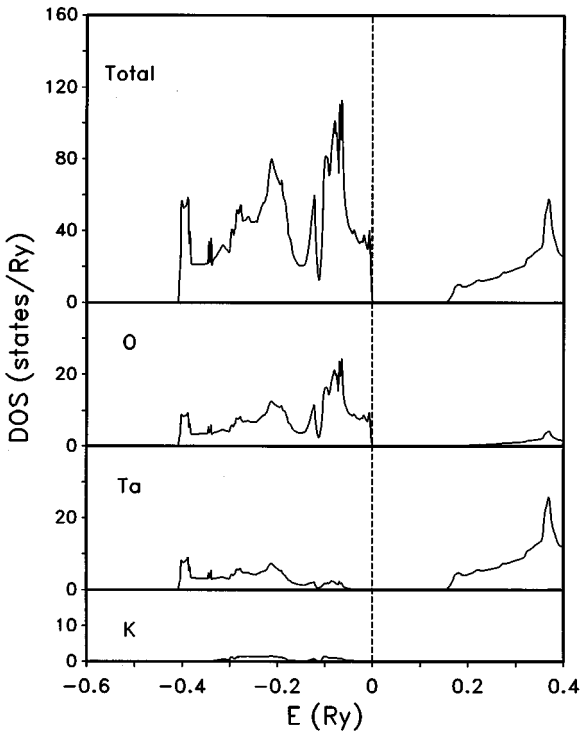

FIG. 2. Total electronic DOS for $KTaO_3$ and projections on the LAPW spheres. The projections are on a per atom basis, with sphere radii of 2.0 a.u., 1.9 a.u., and 1.443 a.u. for K, Ta, and O, respectively. Note that the projections do not sum to the total DOS since some weight is in the interstitial region.

Calculations for $KTaO_3$ at the 0.8% larger lattice parameter of $KNbO_3$, do not significantly change the above differences showing that they are not due to the very slightly smaller O-O separation in the tantalate. Rather they may be understood as due to the approximately 0.5 eV higher binding energy of the d orbitals in Nb relative to Ta.[30] This corresponds well with the 0.6 eV increase in band gap, which may be regarded as due to a raising of the $5d$ derived conduction bands. This also favors somewhat increased ionicity; any increase in the O charge would increase direct O-O interactions. The lower $6s$ state of Ta relative to the $5s$ state of Nb favors increased indirect O-O interactions in the valence band of the tantalate. Relative to the valence band maximum, the O $1s$ core level is shifted to 0.1 eV lower binding energy in $KTaO_3$ relative to $KNbO_3$. The higher d binding energy in the niobate favors greater covalency since the d and p orbitals are then closer in energy. However, the smaller $4d$ orbital radius as compared with the $5d$ orbital radius favors greater covalency in the tantalate. Based on the very similar dispersions of the d-p hybridized bands, these two effects nearly cancel.

ZONE CENTER PHONONS

Two symmetries are allowed for Γ point phonons in the perovskite structure. These are triply degenerate Γ_{15} and Γ_{25} modes. These are three Γ_{15} modes, not counting the acoustic branches. These infrared active branches are split into longitudinal and transverse optic modes. In the present calculation, the wave vector is exactly zero and periodic, zero macroscopic field boundary conditions are applied, so that only the transverse optic phonons are calculated. The symmetry of the Raman active Γ_{25} mode prohibits a macroscopic electric field.

The Γ_{25} frequency was calculated by determining the total energy as a function of the mode displacement in a tetragonal symmetry cell. The frequency was then determined by the quadratic coefficient of the energy as a function of displace-

TABLE I. Calculated frequencies and displacement patterns for $KTaO_3$. The polarization (eigen)vectors may be obtained by multiplying by the square roots of the masses.

	Frequency (cm^{-1})		Displacement pattern				
	Calc.	Expt.	K	Ta	O1	O2	O3
Γ_{15}	80	24,[a]81[b]	0.017	−0.037	0.118	0.128	0.128
Γ_{15}	172	197,[a]199[b]	0.146	−0.021	−0.036	−0.042	−0.042
Γ_{15}	528	546[b]	0.002	0.007	−0.208	0.098	0.098
Γ_{25}	264	274[a]	0.000	0.000	0.000	0.177	−0.177

[a]Ref. 6 at low temperature.

[b]Ref. 31, hyper-Raman scattering at room temperature.

ment. More specifically, the cubic perovskite structure was defined as a simple cubic cell with K at the corners, Ta at the body centers, and O on the face centers. The displacements for the Γ_{25} mode were opposite z-direction displacements of the O ions on the X and Y faces of the cube.

Determination of the three independent Γ_{15} modes is more difficult since the polarization vectors are not determined by symmetry. To obtain these, the atomic forces were calculated for several different displacement patterns within a rhombohedral symmetry cell consistent with the ground state structure of $KNbO_3$. Since forces are linear in the displacements, rather than quadratic as the energy is, it was practical to perform the calculations using very small displacements, in all cases less than 0.05 Å, so that anharmonicity could be neglected. The dynamical matrix was fitted to these force calculations, and then diagonalized to obtain the phonon frequencies and eigenvectors. These are given in Table I along with experimental data. The agreement is best for the high frequency modes and worst for the low frequency ''ferroelectric'' mode, which is 56 cm^{-1} too high. This trend is to be expected since the frequencies are proportional to square roots of the calculated energies and forces (constant accuracy in the force and energy calculations then yields errors proportional to the inverse of the frequency).

Qualitatively, the ''ferroelectric'' mode is found to be stable (real frequency), in agreement with experiment. This may seem more satisfactory than the small imaginary frequency of 61i found by P. However, it should be emphasized that the difference from the experimental frequency of 24 cm^{-1} is roughly the same in the two calculations, and that taking account of the small frequencies involved, the errors in the calculated energies at small displacements needed to account for these differences are extremely minor. The differences in the displacement pattern for this mode are more significant.

As mentioned, P found that at their experimental lattice parameters both $KNbO_3$ and $KTaO_3$ are unstable against displacement of the B site transition metal atom alone. This is reflected in the displacement pattern of the unstable mode. To illustrate this effect, one may take the K ion as fixed (note that one need not use center of mass coordinates for an unstable mode), and normalize the B site cation displacement to be 1.0. In these coordinates the displacement pattern of the unstable mode obtained by P is (0.00,1.00,−0.07,0.10,0.10) in the order of K, Ta, O1, O2, O3 as in Table I. Thus in the calculations of P the unstable mode consists of an almost pure Ta displacement. In the same coordinates, the displacement pattern of the corresponding mode in the present calculations is (0.00,1.00,−1.89,−2.08,−2.08), showing large displacements of the O octahedra relative to the A site K lattice in addition to the Ta displacement. This is in qualitative accord with the experimental rhombohedral structure of $KNbO_3$, which written in the same way is (0.00,1.00,−1.56,−1.32,−1.32). The displacement pattern obtained by Perry *et al.* from fitting their neutron scattering data for $KTaO_3$ is (0.00,1.00,−1.78,−2.12,−2.12), which is in good agreement with the present results.

SOFT MODE ENERGETICS

The calculated energetics of the soft modes of $KTaO_3$ and $KNbO_3$ at their experimental volumes are shown in Fig. 3. This figure shows the energy per formula unit as a function of the relative displacement of the transition metal with respect to the oxygen octahedra. As mentioned, the LDA yields an unstable ferroelectric mode in $KNbO_3$. In contrast the lowest frequency mode is stable in $KTaO_3$.

In both $KNbO_3$ and $KTaO_3$ there is considerable anharmonicity. The soft mode energetics of $KTaO_3$ are well fit

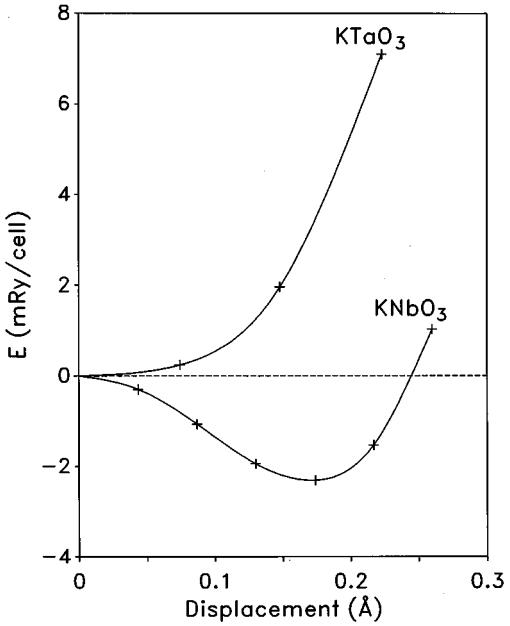

FIG. 3. Energy vs displacement for the ''ferroelectric'' mode in $KTaO_3$ and $KNbO_3$ (Ref. 11). The displacements are the shifts of the transition metal ion with respect to the center of mass of the oxygen octahedra. Note that relative to the K ion, the largest displacements in this mode are those of the oxygen ions.

over the range shown in Fig. 3 by a polynomial with quadratic and quartic coefficients of 0.48 eV/Å^2 and 30 eV/Å^4, respectively.

Yu and co-workers[14] have shown that at least in $KNbO_3$ this mode stiffens rapidly as the wave vector moves away from the zone center along the polarization vector. Presumably a similar stiffening occurs in $KTaO_3$. This strong wave vector dependence is clearly inconsistent with simple Einstein-like models, and accordingly precludes quantitative calculations of its temperature dependence based on simple treatments. Quantitative studies will require construction of lattice dynamical Hamiltonians containing at least the anharmonicity and the dispersion away from the zone center.

Nonetheless, it is clear that the strong quartic term implies strong positive temperature dependence of the frequency as observed. At energies corresponding to room temperature, the energetics are already dominated by the quartic term, and the effective force constant ($2\delta E/x^2$) corresponds to a frequency of 125 cm^{-1}, which is of the same order as the experimentally observed stiffening from 24 cm^{-1} to 81 cm^{-1}.

CONCLUSIONS

LDA calculations have been used to study the zone center phonons of $KTaO_3$. Combined with previous studies of $KNbO_3$, the following emerge: (1) Phonon frequencies and eigenvectors in good agreement with experimental measurements are obtained; (2) the LDA correctly predicts ferroelectric behavior in $KNbO_3$ and the absence of ferroelectricity in $KTaO_3$; (3) the strong temperature dependence of the soft mode in $KTaO_3$ is at least qualitatively described by the LDA; and (4) the ''ferroelectric'' modes are particularly sensitive to the chemistry of the B site cation and other effects such as lattice parameter. The above hold for calculations at the experimental cell volumes. The high sensitivity of the ferroelectric modes to the volume makes the small LDA errors in the lattice parameter significant. Nonetheless, the present results imply that LDA calculations should be a very useful tool in describing the KTN system.

ACKNOWLEDGMENTS

The author is thankful for numerous helpful discussions with L. L. Boyer, R. Yu, and H. Krakauer. This work was supported by the Office of Naval Research. Computations were performed using computers at the DoD Maui High Performance Computing Center and the Arctic Region Supercomputing Center.

[1] M. E. Lines and A. M. Glass, *Principles and Applications of Ferroelectrics and Related Materials* (Clarendon, Oxford, 1977).
[2] A. W. Hewat, J. Phys. C **6**, 2559 (1973).
[3] S. H. Wemple, Phys. Rev. **137**, A1575 (1965).
[4] C. H. Perry and T. F. McNelly, Phys. Rev. **154**, 456 (1967).
[5] P. A. Fleury and J. M. Worlock, Phys. Rev. **174**, 613 (1968).
[6] C. H. Perry, R. Currat, H. Buhay, R. M. Migoni, W. G. Stirling, and J. D. Axe, Phys. Rev. B **39**, 8666 (1989).
[7] Y. Yacobi, A. Agranat, and I. Ohana, Solid State Commun. **45**, 757 (1983).
[8] U. T. Hochli, H. E. Weibel, and L. A. Boatner, J. Phys. C **12**, L562 (1979).
[9] W. Kleemanm, S. Kutz, F. J. Shafer, and D. Rytz, Phys. Rev. B **37**, 5856 (1988).
[10] D. J. Singh and L. L. Boyer, Ferroelectrics **136**, 95 (1992).
[11] D. J. Singh, Ferroelectrics **164**, 143 (1995).
[12] A. V. Postnikov, T. Neumann, G. Borstel, and M. Methfessel, Phys. Rev. B **48**, 5910 (1993).
[13] A. V. Postnikov, T. Neumann, and G. Borstel, Ferroelectrics **164**, 101 (1995).
[14] R. Yu and H. Krakauer, Phys. Rev. Lett. **74**, 4067 (1995); R. Yu, C. Z. Wang, and H. Krakauer, Ferroelectrics **164**, 161 (1995).
[15] R. D. King-Smith and D. Vanderbilt, Phys. Rev. B **49**, 5828 (1994).
[16] W. Zhong, R. D. King-Smith, and D. Vanderbilt, Phys. Rev. Lett. **72**, 3618 (1994).
[17] W. Zhong and D. Vanderbilt, Phys. Rev. Lett. **74**, 2587 (1995).
[18] R. E. Cohen and H. Krakauer, Phys. Rev. B **42**, 6416 (1990).
[19] R. E. Cohen, Nature **358**, 136 (1992).
[20] R. E. Cohen and H. Krakauer, Ferroelectrics **136**, 65 (1992).
[21] R. Comes, M. Lambert, and A. Guinier, Solid State Commun. **7**, 589 (1969).
[22] D. Singh, Phys. Rev. B **43**, 6388 (1991).
[23] O. K. Andersen, Phys. Rev. B **12**, 3060 (1975).
[24] S. H. Wei and H. Krakauer, Phys. Rev. Lett. **55**, 1200 (1985); D. J. Singh, *Planewaves, Pseudopotentials and the LAPW Method* (Kluwer Academic, Boston, 1994).
[25] L. Hedin and B. I. Lundqvist, J. Phys. C **4**, 2064 (1971).
[26] R. Yu, D. Singh, and H. Krakauer, Phys. Rev. B **43**, 6411 (1991).
[27] R. Comes and G. Shirane, Phys. Rev. B **5**, 1886 (1972).
[28] H. H. Barret, Phys. Lett. **26A**, 217 (1968).
[29] T. Neumann, G. Borstel, C. Scharfschwerdt, and M. Neumann, Phys. Rev. B **46**, 10 623 (1992).
[30] W. A. Harrison, *Electronic Structure and the Properties of Solids* (Freeman, San Francisco, 1980).
[31] H. Vogt and H. Uwe, Phys. Rev. B **29**, 1030 (1984).